Heliyon 10 (2024) e27371

Contents lists available at ScienceDirect

Heliyon

journal homepage: www.cell.com/heliyon

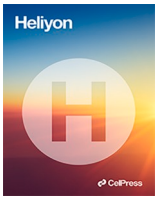

Research article

Modification of ibuprofen to improve the medicinal effect; structural, biological, and toxicological study

Mst Mahfuza Rahman [a,b,*], Mst Farhana Afrin [c], Cai Zong [b], Gaku Ichihara [b], Yusuke Kimura [b], Md Anamul Haque [a], Mir Imam Ibne Wahed [d]

[a] Department of Pharmacy, Faculty of Science, Comilla University, Cumilla, 3506, Bangladesh
[b] Department of Occupational and Environmental Health, Faculty of Pharmaceutical Sciences, Tokyo University of Science, Japan
[c] Department of Applied Chemistry, Graduate School of Engineering, Mie University, Tsu, Mie 514-8507, Japan
[d] Department of Pharmacy, Faculty of Science, University of Rajshahi, Rajshahi, 6205, Bangladesh

ARTICLE INFO

Keywords:
Ibuprofen
Cyclooxygenase
Molecular docking
ADMET
PASS prediction

ABSTRACT

Ibuprofen is classified as a non-steroidal anti-inflammatory drug (NSAID) that is employed as an initial treatment option for its non-steroidal anti-inflammatory, pain-relieving, and antipyretic properties. However, Ibuprofen is linked to specific well-known gastrointestinal adverse effects like ulceration and gastrointestinal bleeding. It has been linked to harmful effects on the liver, kidney, and heart. The purpose of the study is to create novel and potential IBU analogue with reduced side effects with the enhancement of their medicinal effects, so as to advance the overall safety profile of the drug. The addition of some novel functional groups including CH3, F, CF3, OCF3, Cl, and OH at various locations in its core structure suggestively boost the chemical as well as biological action. The properties of these newly designed structures were analyzed through chemical, physical, and spectral calculations using Density Functional Theory (DFT) and time-dependent DFT through B3LYP/6-31 g (d,p) basis set for geometry optimization. Molecular docking and non-bonding interaction studies were conducted by means of the human prostaglandin synthase protein (PDB ID: 5F19) to predict binding affinity, interaction patterns, and the stability of the protein-drug complex. Additionally, ADMET (Absorption, Distribution, Metabolism, Excretion, and Toxicity) and PASS (Prediction of Activity Spectra for Substances) predictions were employed to evaluate the pharmacokinetic and toxicological properties of these structures. Importantly, most of the analogues displayed reduced hepatotoxicity, nephrotoxicity, and carcinogenicity in comparison to the original drug. Moreover, molecular docking analyses indicated improved medicinal outcomes, which were further supported by pharmacokinetic calculations. Together, these findings suggest that the modified structures have reduced adverse effects along with improved therapeutic action compared to the parent drug.

1. Introduction

Ibuprofen or 2- [4-(2-methyl propyl) phenyl] propanoic acid is a non-steroidal anti-inflammatory drug (NSAID) that is derived from propionic acid. Generally, at lower over-the-counter doses (800–1200 mg/day), Ibuprofen (IBU) is prescribed for alleviating mild pain

* Corresponding author. Department of Pharmacy, Faculty of Science, Comilla University, Cumilla, 3506, Bangladesh. Department of Occupational and Environmental Health, Faculty of Pharmaceutical Sciences, Tokyo University of Science, Japan.
E-mail address: mahfuza@cou.ac.bd (M.M. Rahman).

https://doi.org/10.1016/j.heliyon.2024.e27371
Received 28 September 2023; Received in revised form 27 February 2024; Accepted 28 February 2024
Available online 5 March 2024

and inflammation, such as headaches, muscle aches, toothaches, fever, backaches, and menstrual cramps. It has been used as a first line non-steroidal anti-inflammatory, analgesic, and antipyretic agent. It is a non-selective cyclooxygenase enzymes (COX-1 and COX-2) inhibitor that works by the inhibition of prostaglandin synthesis [1]. Due to its anti-inflammatory properties IBU is occasionally used for the treatment of acne, and in Japan, it is available in topical form for adult acne treatment [2,3]. Additionally, ibuprofen, like other NSAIDs, is potentially helpful in managing severe orthostatic hypotension (low blood pressure upon standing [4]. However, the role of NSAIDs, including ibuprofen, in preventing and treating Alzheimer's disease remains uncertain [5,6]. Studies have produced mixed results in this regard. Furthermore, researchers from Harvard Medical School reported in the journal Neurology that IBU may offer neuroprotective effects that reduce the risk of developing Parkinson's disease [7]. Furthermore, IBU can also be used in the treatment of cancer [8].

Besides its beneficial effects, it has some potential side effects like other NSAIDs. IBU can upsurge the jeopardy of heart attack or stroke in people with or without heart disease or the risk issues for heart disease. It has been linked to negative impacts on the kidneys and liver, and these effects seem to be influenced by the dosage, concurrent medications, and the specific group of patients [9,10]. Occasionally, individuals using IBU have experienced severe skin circumstances like Stevens–Johnson syndrome and toxic epidermal necrolysis [11,12]. Moreover, at elevated doses, similar to other NSAIDs, IBU can lead to significant gastrointestinal problems and potentially trigger adverse cardiovascular events [13–18]. IBU can also worsen asthma [19].

Consequently, for diminishing the side effects with appropriate therapeutic action, alternatives of IBU have immediately required. The aim of the current study is to explore the alternatives that possess distinct and advantageous medicinal effects especially analgesic and antipyretic actions with reduced side effects to resolve this problem. Several research endeavors have been undertaken with the intention of identifying substitutes that fulfill some of these specific medicinal goals. Notably, the ongoing studies distinguish themselves from previous studies and have revealed several encouraging outcomes. Existing studies have been shown on anti-inflammatory and pharmacological properties of IBU and some of its derivatives by means of DFT and molecular docking tactics. The alteration of the propionic acid, aryl and/or the isobutyl moieties of ibuprofen has been observed to strengthen the anti-inflammatory, hepatotoxic and molecular properties of the drug candidates [20]. Also, one study was performed to evaluate in silico ibuprofen with potential anti-inflammatory activity via molecular docking with the COX-2 receptor (PDB ID: 4PH9) [21]. Modifying current drugs offers an easy means to quickly progress new drugs with better action and overcome difficulties like resistance and allergies related to existing ones. Computer aided drug design (CADD) is a modern technique of emerging new therapeutic lead compounds. It is a time saving method and it aids in understanding experimental results and enquiries into the mechanism and atomistic facts of molecules and receptors. Furthermore, this approach is highly cost-effective and straightforward, offering a means to discover superior compounds with targeted effects while minimizing adverse effects on both human health and the environment [22,23]. Density Functional Theory (DFT) is a widespread quantum chemical technique applied to examine the molecular properties [24]. Molecular docking supports to forecast the interaction of molecules (ligand) in the active site of the protein (receptor) [25]. It is also used to recognize various binding manners in a protein binding site [26]. Inspecting the pharmacokinetics benefits in foreseeing the effect, fate and safety of a compound after administration in human body. The alteration of a chemical structure brings about substantial changes in the compound's physicochemical, spectral, biological, and pharmacokinetic characteristics. This transformation holds promise in selecting viable alternatives for subsequent investigations (Fig. 1). In this context, a variety of distinct functional groups (such as CH3, F, CF3, OCF3, Cl, and OH) were introduced at the R1 and R2 positions of the core structure. Out of over 40 tested derivatives, a subset of 18 derivatives has been identified as notably more favorable. These specific analogues display enhanced chemical, biological, and medicinal attributes, presenting a valuable foundation for the design of novel potential candidates with better therapeutic effects and abridged adverse effects. Additionally, the PASS forecast information exposed that the potential candidate showcased fewer adverse effects in the majority of the modified analogues compared to the original IBU. As a result, it can be concluded that this study holds significant promise in the development of new potential IBU candidates with diminished side effects.

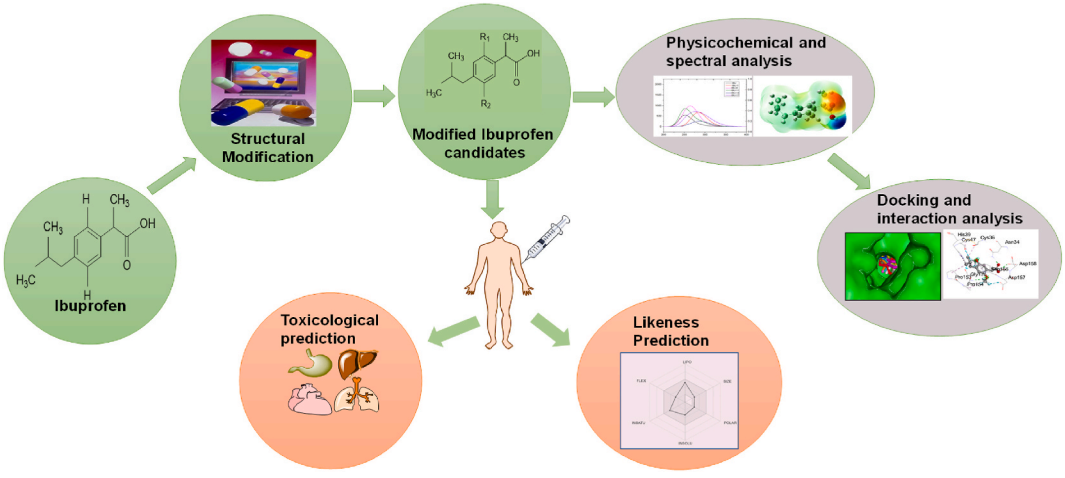

Fig. 1. Flow diagram of research methodology.

This study facilitates the development of a novel drug with maximum clinical safety and efficacy. Nevertheless, some future studies and experimental validations such as synthesis and chemical characterization, biological assay using in vitro and in vivo models to predict and measure these properties of the designed drugs, investigation of acute and chronic toxicities, dose-response studies, formulation studies that should be performed to evaluate the safety, and efficacy of the designed drug candidates.

2. Materials and methods

2.1. Geometry optimization

In the present era, computational methods are gaining increasing prominence and popularity in the realm of drug discovery and development. These tools allow the prediction of formerly unknown and uncharacterized properties of new compounds. This can be accomplished without the prerequisite of expensive laboratory experiments, as computational methods allow for the straightforward prediction of geometrical, molecular orbital, thermodynamic, spectral, and various other biological attributes. The initial structure and all analogues were generated using Gaussian 09 W Revision D.01 [27]. For optimization in the gas phase, Density functional theory (DFT) with the B3LYP [28], and 6-31G (d, p) [29] basis set was employed. Amber potential was utilized for molecular dynamics and conformational searches to identify the lowermost energy and most firm conformer. This was done by means of Gabedit software (version 2.5.0) software [30]. Moreover, TD-DFT projections were conducted to inspect the electronic transitions of the compounds. The attributes of the Frontier Molecular Orbitals, specifically ϵHOMO (Highest Occupied Molecular Orbital) and ϵLUMO (Lowest Unoccupied Molecular Orbital), were computed using the same level of theory. Following this, the HOMO-LUMO gap, hardness (η), softness (S), chemical potential (μ), electronegativity (χ), and electrophilicity (ω) were determined based on the Parr and Pearson interpretation of DFT, as well as Koopmans' theorem. These calculations were performed by means of the subsequent equations [31].

$$\text{Gap}\ (\Delta E) = [\varepsilon\text{LUMO-}\varepsilon\text{HOMO}] \tag{1}$$

$$\eta = \frac{[\varepsilon\text{LUMO-}\ \varepsilon\text{HOMO}]}{2} \tag{2}$$

$$S = \frac{1}{2\eta} \tag{3}$$

$$\mu = \frac{[\varepsilon\text{LUMO} + \varepsilon\text{HOMO}]}{2} \tag{4}$$

$$\chi = -\frac{[\varepsilon\text{LUMO} + \varepsilon\text{HOMO}]}{2} \tag{5}$$

2.2. Preparation of protein, molecular docking, and interaction calculation

The 3D crystal structure of human cyclooxygenase-2 (PDB ID: 5F19) [32] was obtained in pdb form from protein data bank (PDB), an online data archive [33]. To prepare the protein chain, heteroatoms and water molecules were removed using Discovery Studio Visualizer 2021 software and after this, energy minimization using the conjugate gradient technique was employed which supports to eradicate unfavorable contacts among protein molecules. Swiss-PdbViewer software (Version 4.1.0) was used for this purpose (Version 4.1.0) software [34]. Subsequently, the improved protein structures were used for molecular docking experiments with human prostaglandin synthase protein (5F19) as the macromolecule and drugs as ligands. This process was facilitated by PyRx software package (Version 0.8) [35]. For flexible docking, a grid box with dimensions of 64.8642 Å along the x-direction, 73.2984 Å along the y-direction, and 57.9414 Å along the z-direction was set up, covering the entire protein. To assess nonbonded interactions and visualize the docking outcomes, Discovery Studio Visualizer 2021 was employed. This software was also used to analyze and interpret the results of the molecular docking. Also, neural networks are very currently very promising model which can be employed in molecular docking studies to predict the binding affinity of a drug candidate to its target protein. This model helps in understanding the strength of the interaction between a drug and its intended target [36]. The higher binding interaction between the complexes reflects the improved intermolecular forces. The lowermost binding energy stabilizes the complex [37].

2.3. Molecular dynamics simulation

Molecular dynamics simulation is commonly employed to authenticate the findings of molecular docking and to explore the stability of protein-ligand complexes [38,39]. In this study, Normal Mode Analysis (NMA) dynamics simulation was conducted specifically for the C-α atoms of the receptor proteins. This simulation was carried out with the iMODS (https://imods.iqfr.csic.es/) server [40].

2.4. ADMET, biological activities and prediction of drug likeness

Absorption, Distribution, Metabolism, Excretion, and Toxicity (ADMET) specifications contribute a crucial role in the field of drug

discovery. In this study, the ADMET profile was predicted using the admetSAR online server (http://lmmd.ecust.edu.cn/admetsar1/predict/) [41]. Additionally, the PASS (Prediction of Activity Spectra for Substances) online database (http://www.way2drug.com/passonline/) [42] was utilized to predict the activity profiles of the drug-like compounds based on their structural formulas. This program aids in forecasting the potential biological activities of the compounds. The SwissADME web means was employed to forecast the biological and drug-likeness characteristics of the compounds [43]. The outcomes of ADMET, PASS, and drug-likeness predictions for all investigated compounds are outlined in Table 4, Table 5, and Table 6, respectively. To provide input for ADMET and PASS prediction, a Simplified Molecular Input Line Entry System (SMILES) was produced by means of an online server (https://cactus.nci.nih.gov/translate/).

3. Result and discussion

3.1. Thermodynamic study

The crucial notions of free energy, enthalpy, and dipole moment are essential for elucidating tendencies related to molecular associations and reactions. The free energy value can anticipate the extemporaneity of a chemical reaction and the constancy of the resulting products [44]. The free energy data signifies the level of spontaneity in the adsorption method, with a negative value indicating the favorable extemporaneity of the reaction [45]. Amongst the 18 considered analogues, 6 diverse functional groups have been calculated by locating them at three dissimilar places. IBU (depicted in Fig. 2) possesses a free energy value of −656.491 Hartree. In contrast, all the generated analogues exhibit comparatively higher free energy values. Among these, IBU-9, IBU-12, IBU-13, IBU-14, and IBU-15 demonstrate significantly elevated free energy values of −1330.555, −1480.884, −1575.696, −1116.095, and −1575.693 Hartree, respectively. This is attributed to the incorporation of CF3, OCF3, and Cl functional groups into the R1 and R2 positions of the core structure (**Table 1**). The trend of increasingly negative data indicates that these structures are progressively becoming more stable. In the presence of added electronegative atoms F and Cl, IBU-9, IBU-12, IBU-13, IBU-14, and IBU-15 have the highest free energy and enthalpy values.

The dipole moment is a crucial factor in predicting both the dielectric possessions and chemical characteristics of a solvent [46]. It promotes the polarity, binding affinity, and non-bonding interactions within drug-protein complexes through the formation of hydrogen bonds [47]. IBU exhibits a dipole moment value of 1.516 Debye. However, with the exception of IBU-8, IBU-14, IBU-15, and IBU-18, all the analogues display higher dipole moment values than IBU. A higher dipole moment indicates the molecule's strong affinity, propensity for hydrogen bond formation, and increased potential for intermolecular interactions. Within the set of 18 compounds, IBU-7 (approximately 3.541 Debye) and IBU-11 (3.098 Debye) exhibited notably high dipole moment data, largely owing to the incorporation of CF3 and OCF3 functional groups in the R1 position. Moreover, the dipole moment values also vary based on the distinct locations of the same functional group.

3.2. Molecular orbital analysis

The HOMO and LUMO energies, gap, hardness, softness, chemical potential, and electronegativity of all drugs are shown in Table 2. HOMO and LUMO energy calculations can anticipate chemical reactivity, softness, chemical potential, and the shift of electrons between ground and excited states. The uppermost occupied molecular orbital (HOMO) and lowermost unoccupied molecular orbital (LUMO), known as the frontier molecular orbitals, govern how a molecule interacts with other substances [48]. The magnitude of HOMO-LUMO gap impacts the data of chemical softness, hardness, chemical potential, and electronegativity. A wider HOMO-LUMO gap recommends lower chemical reactivity and increased kinetic stability. This is due to the reluctance of the addition of electron to a higher-energy LUMO and electron elimination from a lower-energy HOMO [49]. A small HOMO-LUMO gap designates reduced kinetic stability and higher chemical softness. This is why transitions are preferred when the HOMO-LUMO gap is smaller [50]. In the present examination, IBU exhibits a HOMO-LUMO gap of 6.112 eV. In contrast, IBU-18 demonstrates the narrowest energy gap (5.161 eV) along with the highest softness value (0.194 eV), indicating greater chemical activity compared to the other compounds (as depicted in Fig. 3). Nearly all of the IBU analogues exhibit narrower HOMO-LUMO gaps and elevated chemical softness data when compared to the original IBU compound.

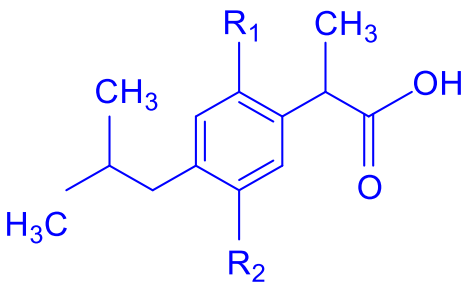

Fig. 2. Chemical structure of Ibuprofen (IBU).

Table 1
Chemical structures, Molecular formula (MF), molecular weight (MW), enthalpy, free energy (Hartree), and dipole moment (Debye) of IBU, and its newly designed analogues.

Name	R1	R2	MF	MW	Enthalpy (Hartree)	Free energy (Hartree)	Dipole moment
IBU	H	H	$C_{13}H_{18}O_2$	206.281	−656.431	−656.491	1.516
IBU-1	CH_3	H	$C_{14}H_{20}O_2$	220.307	−695.720	−695.784	1.742
IBU-2	H	CH_3	$C_{14}H_{20}O_2$	220.307	−695.718	−695.782	1.843
IBU-3	CH_3	CH_3	$C_{15}H_{22}O_2$	234.334	−735.007	−735.074	1.640
IBU-4	F	H	$C_{13}H_{17}O_2F$	224.271	−755.668	−755.732	1.928
IBU-5	H	F	$C_{13}H_{17}O_2F$	224.271	−755.671	−755.734	2.390
IBU-6	F	F	$C_{13}H_{16}O_2F_2$	242.262	−854.909	−854.973	1.808
IBU-7	CF_3	H	$C_{14}H_{17}O_2F_3$	274.279	−993.454	−993.522	3.541
IBU-8	H	CF_3	$C_{14}H_{17}O_2F_3$	274.279	−993.454	−993.523	1.063
IBU-9	CF_3	CF_3	$C_{15}H_{16}O_2F_6$	342.277	−1330.478	−1330.555	1.617
IBU-10	OCF_3	H	$C_{14}H_{17}O_3F_3$	290.278	−1068.672	−1068.744	1.869
IBU-11	H	OCF_3	$C_{14}H_{17}O_3F_3$	290.278	−1068.670	−1068.740	3.098
IBU-12	OCF_3	OCF_3	$C_{15}H_{16}O_4F_6$	374.276	−1480.911	−1480.884	1.565
IBU-13	Cl	H	$C_{13}H_{17}O_2Cl$	240.726	−1116.030	−1116.093	3.318
IBU-14	H	Cl	$C_{13}H_{17}O_2Cl$	240.726	−1116.031	−1116.095	0.525
IBU-15	Cl	Cl	$C_{13}H_{16}O_2Cl_2$	275.171	−1575.627	−1575.693	1.110
IBU-16	OH	H	$C_{13}H_{18}O_3$	222.280	−731.645	−731.709	2.853
IBU-17	H	OH	$C_{13}H_{18}O_3$	222.280	−731.645	−731.708	2.136
IBU-18	OH	OH	$C_{13}H_{18}O_4$	238.280	−806.858	−806.924	1.483

Table 2
Energy (eV) of HOMO, LUMO, energy gap, hardness(η), softness (S) and chemical potential (μ), and electronegativity (χ) of all optimized structures.

Name	εHOMO	εLUMO	gap	η	S	μ	χ
IBU	−6.378	−0.267	6.112	3.056	0.164	−3.323	3.323
IBU-1	−6.249	−0.253	5.996	2.998	0.167	−3.251	3.251
IBU-2	−6.236	−0.244	5.992	2.996	0.167	−3.240	3.240
IBU-3	−6.080	−0.224	5.856	2.928	0.171	−3.152	3.152
IBU-4	−6.461	−0.483	5.978	2.989	0.167	−3.472	3.472
IBU-5	−6.429	−0.489	5.940	2.970	0.168	−3.459	3.459
IBU-6	−6.415	−0.576	5.839	2.920	0.171	−3.495	3.495
IBU-7	−6.753	−0.844	5.908	2.954	0.169	−3.798	3.798
IBU-8	−6.770	−0.780	5.990	2.995	0.167	−3.775	3.775
IBU-9	−7.108	−1.400	5.708	2.854	0.175	−4.254	4.254
IBU-10	−6.723	−0.574	6.149	3.074	0.163	−3.649	3.649
IBU-11	−6.583	−0.609	5.975	2.987	0.167	−3.596	3.596
IBU-12	−6.860	−0.883	5.977	2.988	0.167	−3.872	3.872
IBU-13	−6.541	−0.406	6.135	3.068	0.163	−3.474	−3.474
IBU-14	−6.543	−0.570	5.974	2.987	0.167	−3.556	3.556
IBU-15	−6.563	−0.653	5.910	2.955	0.169	−3.608	3.608
IBU-16	−5.943	−0.186	5.758	2.879	0.174	−3.064	3.064
IBU-17	−5.909	−0.305	5.604	2.802	0.178	−3.107	3.107
IBU-18	−5.413	−0.252	5.161	2.581	0.194	−2.833	2.833

3.3. Molecular electrostatic potential study

The molecular electrostatic potential (MEP) elucidates the spreading of electronic charge and nuclear charge of a molecule in its surrounding space. It also offers insights into the molecule's partial charges, dipole moment, electronegativity, and chemical reactivity [51,52]. The molecular electrostatic potential (MEP) can be used to understand hydrogen bonding and the process of biological gratitude [53]. The MEP also aids in predicting the physicochemical characteristics of a drug-like molecule, allowing it to function as both a hydrogen bond donor and acceptor within its receptor [54]. The intense red color, indicating electron-rich regions, signifies sites favorable for electrophilic attacks due to an abundance of electrons. On the other hand, the deep blue color, representing electron-deficient regions, suggests areas suitable for nucleophilic attacks as they lack electrons. In the MEP map (Fig. 4), the color green signifies regions with zero potential. Within this map, hydrogen molecules exhibit the most positive potential, while oxygen molecules possess the most negative potential. In this ongoing study, IBU showcases electrophilic potential values of −5.481e-2 and +5.481e-2 atomic units (a.u.). Owing to the presence of OH functional groups in the R1 position of the core structure, IBU-16 exhibits the most negative potentiality (−6.489e-2 a.u., deep red) and the highest positive potentiality (+6.489e-2 a.u., deep blue). This implies a heightened likelihood of electrophilic and nucleophilic attacks at the targeted region.

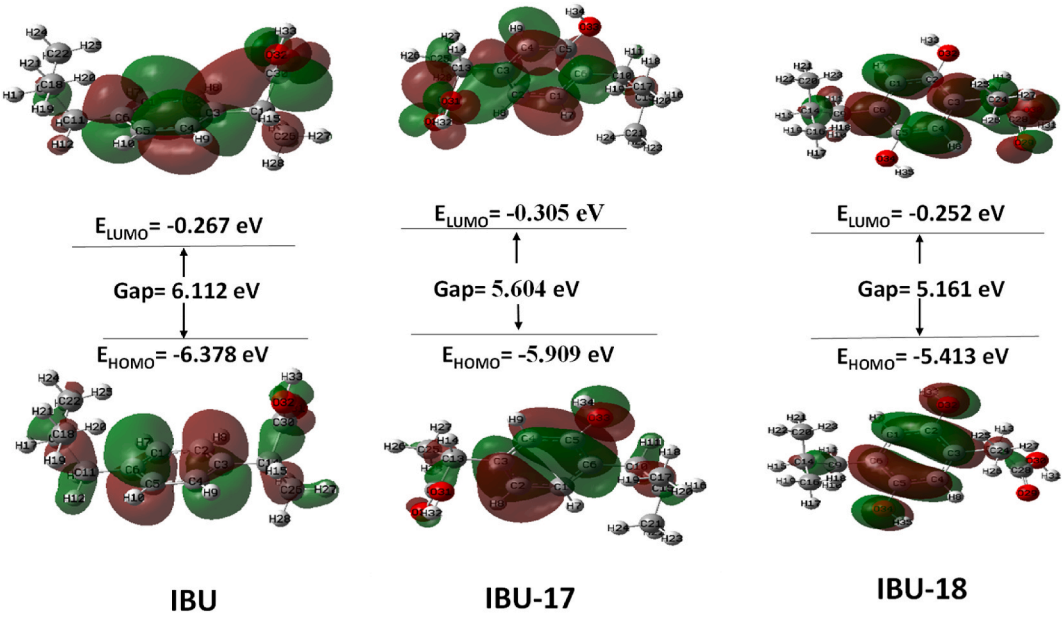

Fig. 3. Frontier molecular orbital (HOMO and LUMO) and related energy of IBU, IBU-17, and IBU-18.

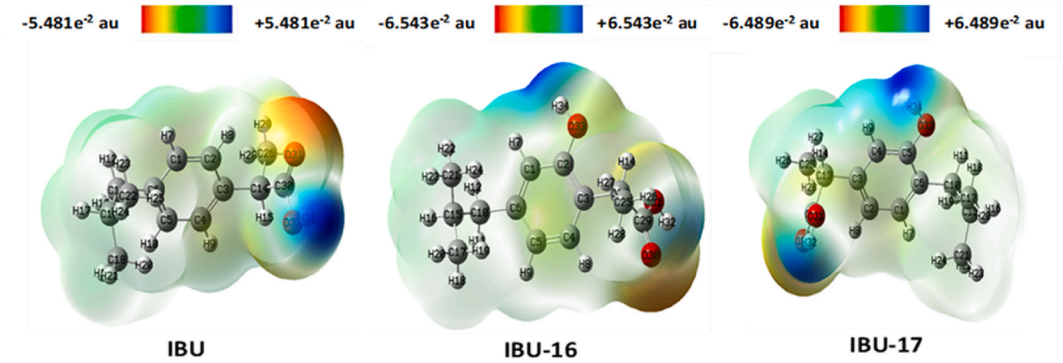

Fig. 4. Molecular electrostatic potential map of IBU, IBU-16, and IBU-17 **(remaining are presented in Fig. S1).**

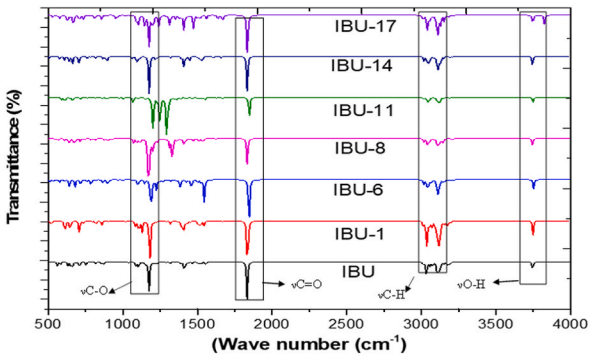

Fig. 5. FT-IR spectra of some selected compounds.

3.4. Vibration frequency analysis

Fourier-transform infrared (FT-IR) spectral analysis is a crucial technique for investigating chemical structures. It confirms the existence of diverse functional groups within a molecule [55]. The FT-IR spectral value of the IBU drug and its analogues are organized and presented in Table S1 and Fig. 5. The FT-IR spectral vibrational frequencies for all compounds are documented within the series of 400–4000 cm-1. The hydroxyl (OH) functional (carbonyl stretching of isopropionic acid group) provides vibration stretching's in the frequency array of 3604–3614 cm^{-1}, and approve the existence of carboxylic OH in these compounds. Also, C═O (carbonyl stretching of isopropionic acid group) group of all modified structures display stretching vibration at the range of 1756–1778 cm^{-1}, whereas parent IBU exhibit at 1763 cm^{-1}. The alteration in the IR band is owing to the existence of the diverse functional groups in a diverse chemical atmosphere that happened owing to the variation of the functional group of IBU. The symmetrical and asymmetric vibrational stretching for C–H functional group of all modified structures is found in the range of 3032–3068 cm^{-1} and 2990-3058 cm^{-1} region whereas parent IBU shows C–H group symmetrical and asymmetric vibrational stretching at 2943 cm^{-1} and 2990 cm^{-1}. These considered consequences are in relatable arrangement with the experimental data (experimental data shows C═O group stretching at 1721 cm^{-1}, C–H group symmetrical and asymmetric vibrational stretching at 2869 cm^{-1} and 3090 cm^{-1} respectively [56]. C–O (stretching of isopropionic acid group) group of the parent IBU displays stretching vibration at 1130.230, whereas all the modified compounds show in the range of 1125–1163 cm^{-1} almost close to the experimental value (1183 cm^{-1}). C–F bond stretching's are found in 1123–1252 cm^{-1} in IBU-7 to IBU-12 compounds. Characteristic vibrational frequency bands are displayed at 1195–1199 cm^{-1} clearly signifying the existence of OCF_3 functional group in IBU-10 to IBU-12 compounds. Another hydroxyl (OH) functional group provides vibration stretching's in the frequency range of 3682–3689 cm^{-1}, and approve the existence of carboxylic OH in IBU-16 to IBU-18 compounds.

3.5. UV–Vis spectral analysis

The uv–visible spectroscopy using time-dependent density functional theory (TD-DFT) calculations were performed for all molecules under investigation to understand the nature of electronic transition within the molecule [57]. In this investigation, the electronic transition bands of all altered structures, including IBU, were computed using the time-dependent (TD)-DFT-B3LYP/631G (d,p) method. The calculated values for absorption peaks (λ_{max}), excitation energies, oscillator strengths (f), and transition assignments for all analogues were compiled and presented in Table S2. Additionally, the UV–Vis spectra for several chosen IBU analogues were graphically represented in Fig. 6. In this present investigation, the supreme absorption wavelengths of altogether the molecules were detected within the array of 200–400 nm in the UV–Vis area. For IBU-18, the absorption maximum was recorded at 343.64 nm in the S0 → S1 excited state, with a configuration alignment of 0.704 (H → L) and an oscillator strength (f) of 0.0139. As IBU-18 demonstrated an absorption peak at an extended wavelength, it has the lowermost energy and is consequently the steadiest amongst all the compounds. Conversely, IBU-3 exhibited the absorption maximum at the shortest wavelength (254.44 nm), resulting in the uppermost energy and the least stability.

3.6. Docking and interactions study

Molecular docking plays a vital role in the process of structure-based drug discovery [58]. The primary objective of docking is to explore the binding affinities of ibuprofen (IBU) and its analogues as prostaglandin inhibitors. In terms of binding characteristics, more negative data specify a more robust binding interaction between the ligands and the receptor protein. In this context (as presented in Table 3), IBU demonstrates a binding affinity of −7.6 kcal/mol. Notably, the majority of the analogues exhibit notably higher binding affinities, except for IBU-2 (−7.1 kcal/mol), IBU-3 (−6.3 kcal/mol), IBU-10 (−6.5 kcal/mol), IBU-12 (−6.8 kcal/mol), IBU-13 (−7.2 kcal/mol), IBU-15 (−7.2 kcal/mol), and IBU-18 (−7.4 kcal/mol). Augmented hydrogen bonding is a key factor contributing significantly to the improvement of the binding affinity between ligands and receptor proteins. Existing literature indicates that hydrogen

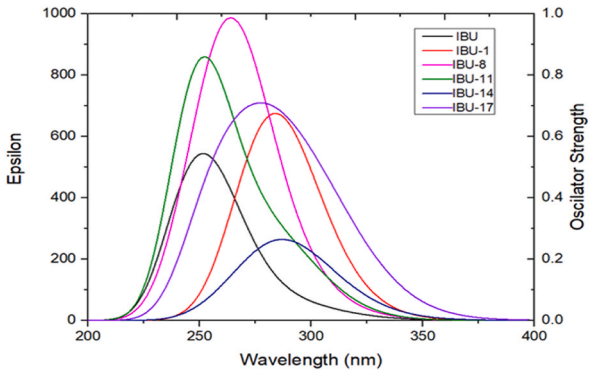

Fig. 6. UV–Visible spectra of some selected IBU analogues.

Table 3
Binding affinity and nonbonding interactions of some selected compounds with the receptor protein (5F19) after molecular docking **(remaining are shown in Table S1)**.

Name	Binding affinity (kcal/mol)	Residue in contact	Interaction type	Bond distance (Å)
IBU	−7.6	ALA527	Conventional Hydrogen Bond	2.74826
		TYR385	Pi-Pi T-shaped	5.19318
		LEU534	Alkyl	4.10583
		LEU384	Alkyl	5.11402
		PHE205	Pi-Alkyl	4.61737
		PHE205	Pi-Alkyl	4.83682
		PHE209	Pi-Alkyl	4.82052
		PHE209	Pi-Alkyl	5.05133
		PHE381	Pi-Alkyl	4.89862
		TYR385	Pi-Alkyl	4.67858
		TYR385	Pi-Alkyl	4.94812
		TRP387	Pi-Alkyl	4.87766
		VAL349	Pi-Alkyl	5.37363
IBU-6	−8.2	LEU531	Conventional Hydrogen Bond	2.63582
		LEU531	Conventional Hydrogen Bond	2.07968
		GLY526	Halogen (Fluorine)	3.1771
		ALA527	Alkyl	3.72924
		LEU352	Alkyl	4.59034
		VAL523	Alkyl	3.89959
		VAL523	Alkyl	3.76144
		PHE518	Pi-Alkyl	5.43936
		VAL349	Pi-Alkyl	5.17746
		LEU352	Pi-Alkyl	5.35548
IBU-8	−8.7	LEU531	Conventional Hydrogen Bond	2.09959
		ALA527	Conventional Hydrogen Bond	2.5647
		PHE529	Conventional Hydrogen Bond	2.38377
		VAL523	Carbon Hydrogen Bond; Halogen (Fluorine)	3.40396
		GLY526	Carbon Hydrogen Bond; Halogen (Fluorine)	3.16116
		MET522	Halogen (Fluorine)	2.84699
		MET522	Halogen (Fluorine)	3.57285
		GLY526	Halogen (Fluorine)	3.56541
		ALA527	Alkyl	3.72828
		LEU352	Alkyl	4.77714
		VAL523	Alkyl	3.87189
		VAL523	Alkyl	3.9882
		MET522	Alkyl	5.26385
		TRP387	Pi-Alkyl	5.32597
		PHE518	Pi-Alkyl	5.23251
		VAL349	Pi-Alkyl	4.95776
		LEU352	Pi-Alkyl	5.18545
IBU-11	−8.4	LEU531	Conventional Hydrogen Bond	2.60075
		LEU531	Conventional Hydrogen Bond	2.23707
		GLY526	Conventional Hydrogen Bond	2.32071
		ALA527	Conventional Hydrogen Bond	3.03655
		PHE529	Conventional Hydrogen Bond	2.12904
		MET522	Halogen (Fluorine)	3.184
		MET522	Halogen (Fluorine)	3.2418
		LEU352	Alkyl	4.31299
		VAL523	Alkyl	4.03049
		VAL523	Alkyl	4.24986
		VAL349	Alkyl	4.61557
		MET522	Alkyl	4.69333
		TYR348	Pi-Alkyl	4.84769
		TYR355	Pi-Alkyl	5.12332
		TRP387	Pi-Alkyl	5.25298
		PHE518	Pi-Alkyl	5.06436
		PHE518	Pi-Alkyl	4.43109
		VAL349	Pi-Alkyl	4.87816
		ALA527	Pi-Alkyl	4.47287

bonds with distances less than 2.3 Å have the potential to substantially enhance binding properties to varying degrees [59]. Furthermore, non-covalent interactions play a vital role as essential parameters in ligand-protein complexes. These interactions are accountable for steadying the drug at the designated target position, thereby increasing drug efficacy and influencing the binding affinity [60]. Non-covalent interactions, including halogen bonds, hydrogen bonds, and hydrophobic interactions, are present in nearly altogether the studied structures involving 5F19 (Fig. 7). In this investigation, significant carbon-hydrogen bonds have been identified with VAL523, GLY526, and PRO86 residues in the derivatives IBU-8, IBU-10, and IBU-17. Conventional hydrogen bonds

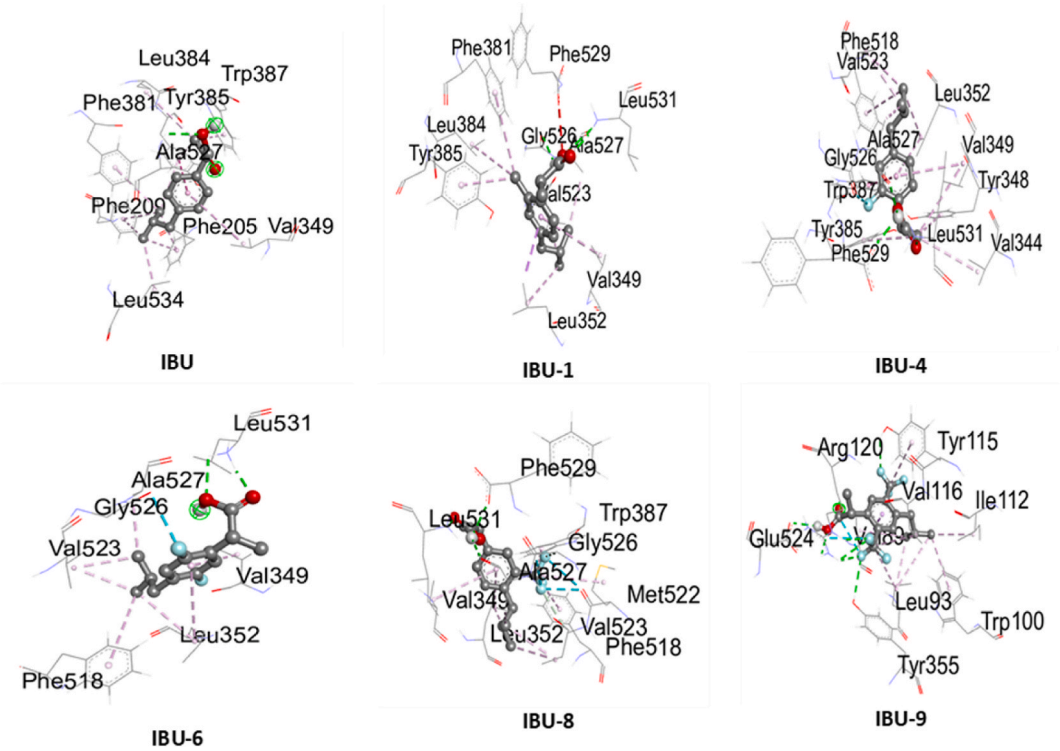

Fig. 7. Nonbonding interactions of IBU, IBU-1, IBU-4, IBU-6, IBU-8, and IBU-9 with the amino acid residues of receptor protein **(remaining are shown in Fig. S2)**.

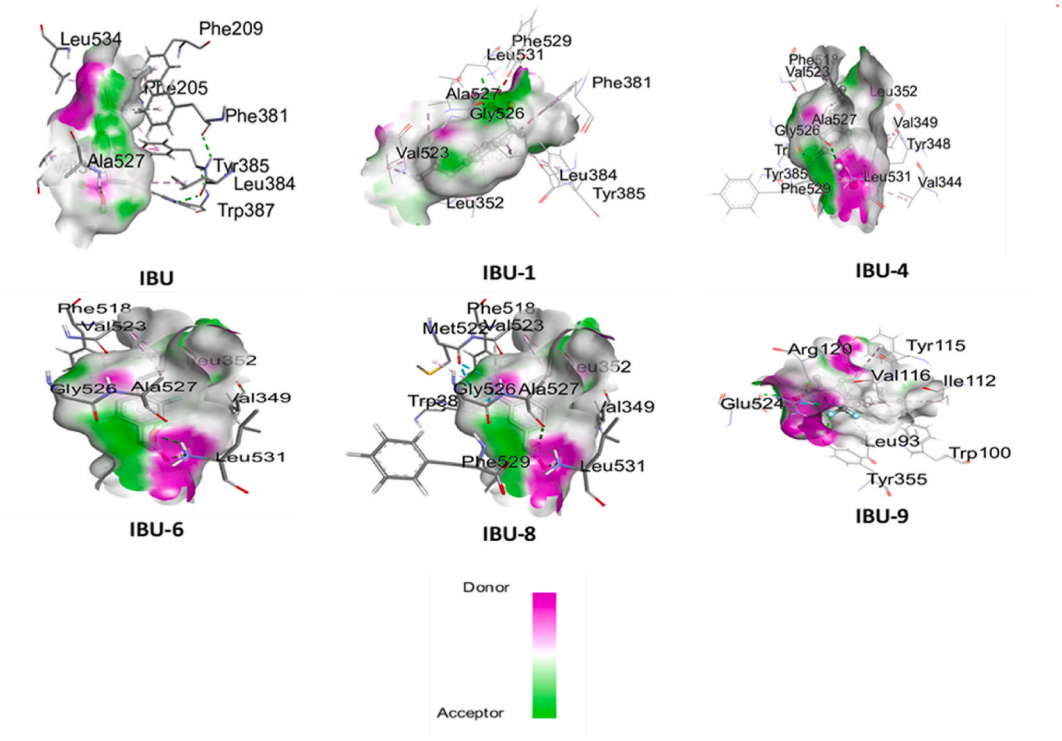

Fig. 8. Hydrogen bond surface of IBU, IBU-1, IBU-4, IBU-6, IBU-8, and IBU-9 with the amino acid residues of receptor protein **(remaining are shown in Fig. S3)**.

(<2.3 Å) are observed in nearly entirely derivatives. Hydrogen bonds play a crucial role in non-bonding interactions and are represented by pink and green colors, indicating hydrogen bond donors and acceptors, respectively (Fig. 8). Furthermore, the halogen bond is comparable in significance to the hydrogen bond and holds a vital function in together chemical and biological schemes [61]. Significant halogen bonds, which have a crucial influence on designing new molecules, are present in the derivatives IBU-4 to IBU-12 involving residues GLY526, MET522, ARG120, and ASP157. Additionally, π-systems hold importance in ligand-protein recognition within biological phenomena. In biological systems, π-bonds contribute substantially to the binding energy [62,63]. In our investigation, nearly all complexes have exhibited Pi-Alkyl interactions with significant amino acid residues. Additionally, a significant Amide-Pi-stacked interaction is observed with GLY526 and ALA527 in the analogues IBU-7, IBU-14, and IBU-15. In this context, Pi-anion interaction is observed in IBU-15 with the PHE529 residue. Furthermore, numerous Pi-Pi-T-shaped interactions are found in IBU-3, IBU-4, and IBU-10 with TRY387 and TYR115 residues. Another notable interaction, Pi-sigma interaction, is identified in the analogues IBU-1, IBU-3, IBU-9, IBU-10, and IBU-18 with the LEU352, VAL89, and VAL349 residues.

3.7. ADMET study

Table 4 presents the outcomes of the AdmetSAR online server's calculations and investigation, with "Admet" standing for absorption, distribution, metabolism, elimination, and toxicity [64]. This calculation has been accomplished to assess the absorption, distribution, metabolism, elimination, and toxicity of both ibuprofen and its improved structures. Indeed, this topic holds great significance in the research and development sectors, especially in the initial stages of drug discovery and development. The ADMET analysis is crucial for exploring all aspects of a potential drug's characteristics [65,66]. In this context, all the constructed structures demonstrate a positive outcome for blood-brain barrier (BBB) criteria, human intestinal absorption (HIA), and Caco-2 permeability. A positive BBB result indicates the potential for these drugs to cross the blood-brain barrier. Nevertheless, due to the risk of possible neurotoxicity and undesirable pharmacological action, BBB permeation should be limited for central nervous system (CNS) drugs [67]. Enhanced human intestinal absorption (HIA) indicates that these compounds have an improved ability to be absorbed in the intestinal tract following oral administration [68].

Furthermore, Caco-2 cells replicate a spectrum of transcellular trails and the metabolic transformation of trial compounds through stating transporter proteins, phase II conjugation enzymes, and efflux proteins. It's noteworthy that all the analogues successfully traverse the Caco-2 monolayer [69]. CYP2C9, a crucial cytochrome P450 enzyme, exhibits no inhibition by all the projected drugs. Inhibition of this enzyme is known to contribute to a variety of adverse drug reactions linked to its activity [70,71]. Approximately 9 out of the 18 anticipated structures are determined to be non-carcinogenic. All the projected structures fall under Category III for acute oral toxicity, implying their safety for oral consumption. Notably, all the projected drugs are classified as P-glycoprotein non-inhibitors, which is significant as P-glycoprotein inhibition could disrupt the absorption, permeability, and retention of the drugs [72]. In the context of cardiac muscle function, the human ether-a-go-go-related gene (hERG) is essential for potassium channel opening. In this study, all the newly developed drugs exhibit a non-inhibitory characteristic for the human ether-a-go-go-related gene (hERG), signifying their safety for the heart muscle. It's important to note that suppressing the hERG gene could potentially lead to arrhythmia or prolonged QT intervals [73]. Approximately 9 out of the 18 compounds are classified as non-carcinogenic, and altogether of them fall into Category III for acute oral noxiousness. This prediction suggests that these derivatives are relatively fewer detrimental than the parental drug (IBU) for oral administration.

Table 4
Pharmacokinetic parameters of all IBU compounds.

Name	BBB	HIA	C2P	PGp-I	CYP4502C9	hERG	Carcinogen	AOT
IBU	+(0.9619)	0.9927	0.8866	NI (0.9705)	NI (0.9305)	0.9734	C (0.5553)	III
IBU-1	+(0.9818)	0.9891	0.8768	NI (0.9307)	NI (0.9153)	0.9380	NC (0.5320)	III
IBU-2	+(0.9728)	0.9931	0.8759	NI (0.9496)	NI (0.9421)	0.9653	NC (0.5621)	III
IBU-3	+(0.9816)	0.9905	0.8647	NI (0.9371)	NI (0.9323)	0.9338	NC (0.5731)	III
IBU-4	+(0.9876)	0.9929	0.8290	NI (0.9362)	NI (0.6736)	0.9405	C (0.5057)	III
IBU-5	+(0.9876)	0.9929	0.8290	NI (0.9362)	NI (0.6736)	0.9405	C (0.5057)	III
IBU-6	+(0.9876)	0.9929	0.8290	NI (0.9362)	NI (0.6736)	0.9405	C (0.5057)	III
IBU-7	+(0.9896)	1.0000	0.7843	NI (0.9292)	NI (0.7950)	0.9200	C (0.5212)	III
IBU-8	+(0.9896)	1.0000	0.7843	NI (0.9292)	NI (0.7950)	0.9200	C (0.5212)	III
IBU-9	+(0.9896)	1.0000	0.7843	NI (0.9292)	NI (0.7950)	0.9200	C (0.5212)	III
IBU-10	+(0.9531)	1.0000	0.7571	NI (0.8650)	NI (0.7113)	0.9084	NC (0.6463)	III
IBU-11	+(0.9531)	1.0000	0.7571	NI (0.8650)	NI (0.7113)	0.9084	NC (0.6463)	III
IBU-12	+(0.9506)	0.9933	0.6875	NI (0.8721)	NI (0.6612)	0.9250	NC (0.6746)	III
IBU-13	+(0.9817)	0.9928	0.8352	NI (0.9692)	NI (0.6691)	0.9541	C (0.5467)	III
IBU-14	+(0.9817)	0.9928	0.8352	NI (0.9692)	NI (0.6691)	0.9541	C (0.5467)	III
IBU-15	+(0.9817)	0.9928	0.8352	NI (0.9692)	NI (0.6691)	0.9541	C (0.5467)	III
IBU-16	+(0.6572)	0.9837	0.8407	NI (0.9700)	NI (0.5691)	0.9487	NC (0.7569)	III
IBU-17	+(0.6252)	0.9946	0.8134	NI (0.9517)	NI (0.8987)	0.9525	NC (0.7967)	III
IBU-18	+(0.6495)	0.9671	0.6590	NI (0.9702)	NI (0.6167)	0.9567	NC (0.8315)	III

BBB= Blood brain barrier, HIA= Human intestinal absorption, C2P= CACO-2 permeability, P-GpI = P-glycoprotein inhibitor, hERG = human Ether-a-go-go Related Gene, AOT = Acute oral toxicity, NI = non-inhibitor, C = carcinogen, NC = non-carcinogen.

Table 5
Predicted biological activity of some selected IBU analogue.

Name	Analgesic	Anti-Inflammatory	Anti-pyretic	Occult bleeding	Hematuria	Aphthous ulcer	Hepatotoxic	Inflammation	Neprho-toxic	Hematotoxic
IBU	0.461	0.901	0.818	0.968	0.812	0.798	0.737	0.718	0.745	0.734
IBU-1	0.395	0.856	0.743	0.936	0.681	0.751	0.686	0.673	0.667	0.678
IBU-2	0.448	0.884	0.879	0.938	0.715	0.751	0.755	0.746	0.721	0.774
IBU-3	0.404	0.867	0.758	0.918	0.662	0.750	0.671	0.677	0.653	0.687
IBU-4	0.433	0.873	0.606	0.928	0.647	0.644	0.497	0.569	0.627	0.482
IBU-5	0.544	0.874	0.682	0.930	0.684	0.644	0.534	0.592	0.715	0.530
IBU-6	0.429	0.871	0.521	0.908	0.627	0.642	0.444	0.528	0.645	0.434
IBU-7	0.486	0.837	0.714	0.919	0.583	0.781	0.550	0.605	0.587	0.508
IBU-8	0.533	0.865	0.851	0.921	0.625	0.781	0.645	0.657	0.653	0.629
IBU-9	0.497	0.847	0.729	0.897	0.560	0.780	0.533	0.600	0.570	0.521
IBU-10	0.510	0.807	0.499	0.929	0.696	0.711	0.657	0.681	0.684	0.548
IBU-11	0.489	0.832	0.648	0.931	0.669	0.711	0.646	0.637	0.645	0.568
IBU-12	0.476	0.814	0.497	0.910	0.679	0.710	0.670	0.642	0.643	0.552
IBU-13	0.362	0.814	0.651	0.945	0.691	0.734	0.720	0.581	0.664	0.662
IBU-14	0.486	0.855	0.722	0.958	0.740	0.735	0.797	0.638	0.730	0.753
IBU-15	0.362	0.814	0.651	0.945	0.691	0.734	0.720	0.581	0.664	0.662
IBU-16	0.377	0.870	0.826	0.936	0.828	0.859	0.858	0.780	0.782	0.786
IBU-17	0.351	0.887	0.927	0.939	0.810	0.859	0.853	0.738	0.760	0.795
IBU-18	0.328	0.876	0.824	0.919	0.817	0.859	0.863	0.745	0.759	0.788

3.8. PASS and prediction of drug-likeness

PASS (Prediction of Activity Spectra for Substances) and drug-likeness forecast are utilized to explore the potential biological activities of various composites by means of the PASS online server [74]. Through structure-activity relationships study, PASS prediction encompasses an extensive array of information regarding the biological effects of over 300,000 compounds. This tool categorizes organic compounds into 4000 different biological activities according to their molecular structural formulas, achieving an accuracy level above 95% [75].

Examining Tables 5 and it becomes evident that IBU and its analogues exhibit diverse outcomes for various properties. Notably, nearly all analogues demonstrate activity as anti-inflammatory agents (with values ranging from 0.814 to 0.901), antipyretic agents (0.499–0.927), and analgesic agents (0.328–0.533). Moreover, the majority of the analogues (excluding IBU-16 and IBU-18) result in lower occurrences of hematuria (presence of blood in urine) compared to IBU.

Once again, the majority of the predicted analogues derived from IBU exhibit a reduction in the effects related to occult bleeding, hematuria (blood in the urine), hepatotoxicity, and gastrointestinal tract inflammation, as opposed to IBU which shows comparatively higher effects in these areas. Furthermore, most of the predicted analogues demonstrate moderately diminished effects (ranging from 0.754 to 0.642) on aphthous ulcers (canker sores) compared to IBU (except for IBU-16, IBU-17, and IBU-18). Additionally, nephrotoxicity is significantly reduced in most of the IBU analogues (ranging from 0.745 to 0.587). Furthermore, nearly all newly designed analogues of IBU (excluding IBU-16, IBU-17, and IBU-18) exhibit markedly reduced hematotoxic effects (ranging from 0.734 to 0.434) compared to the parent compound (IBU). In summary, these analogues demonstrate analgesic, anti-inflammatory, and antipyretic possessions while mitigating adverse responses in the human body. To conclude, the newly developed IBU analogues perform improved results than the original compound in minimizing the harmful action of IBU in the human body.

In drug discovery, drug-likeness can be employed to evaluate the physical and chemical characteristics of the composites and measure their consistency, aiming to ensure that the compounds exhibit features consistent with those of recognized drugs [76]. Indeed, drug-likeness predictions involve the application of rules based on sophisticated machine learning approaches, which have garnered substantial attention and recognition in the study domain [77]. Lipinski's law, also known as the "Rule of Five," was introduced in 1997 and is one of the most established guidelines for determining a molecule's oral activity. These rules encompass five criteria, and if a molecule disrupts two or more of these guidelines, it is generally considered to be not orally active [78]. From Table 6, entirely the correspondents obeyed the drug-likeness law, like Lipinski et al. [79], Ghose et al. [80], Veber et al. [81], Egan et al. [82], and Muegge et al. [83], and contributed the bioavailability score (ranging from 0.56 to 0.85). Contrastingly, IBU-9, IBU-12, IBU-13, and IBU-15 have exhibited violations of one or more distinct laws. The count of hydrogen bond donors and acceptors, considered as molecular descriptors, is utilized to assess the oral bioavailability of drug molecules. Consequently, an extreme number of hydrogen bond donors and acceptors can impact a drug's membrane permeability and partitioning [84]. Lipinski's rule suggests that drug molecules might experience poor absorption or limited membrane permeability if two or more standards are met, as indicated by the subsequent conditions: molecular weight (M.W.) $>$ 500, computed log P value $>$ 5, hydrogen bond donors $>$5, and hydrogen bond acceptors $>$10 [85]. In conclusion, our study on IBU analogues has been undertaken with the goal of addressing the challenges associated with poor drug absorption and permeation.

3.9. Molecular dynamics simulation study

Normal mode analysis (NMA) is a commonly employed technique to depict the communal functional wave of macromolecules. This technique is employed to investigate the pliability and/or resilience of receptor proteins by monitoring variations in bond lengths, angles, dihedral angles, torsions, vibrations, and alterations in shape across different parameters. Interaction index refer to the protein's ability to interact with other molecules, such as ligands, cofactors, or other proteins. The ability for deformation at each of a protein chain's residues is measured through deformability. Indeed, flexibility or the capacity to change shape of the protein chain evaluates the potential for distortion at individual residues along the protein chain. For the 5F19 receptor (Fig. 9 (A)), the highest oscillation was detected for TYR 55. Some medium heights of distortion predisposition were detected for LEU 108, ARG 376, and GLU 486. The covariance map (depicted in Fig. 9(B)) illustrates the connections between amino acid residues through color coding. Correlated interactions are represented in red, uncorrelated interactions in white, and anti-correlated interactions in blue which stands alongside the origin sharp straight line, displays the coupling of the amino acid residues. These patterns are situated alongside the reference line originating from the origin point. Likewise, the elastic network map (as shown in Fig. 9(C)) illustrates pairs of atoms linked by springs. Each dot on the map corresponds to a spring connecting specific atom pairs. Darker gray dots signify stiffer springs, while lighter gray dots indicate more flexible springs.

4. Conclusion

In this study, both IBU and its modified derivatives have been examined to delve into their physical and chemical characteristics or attributes, and their strengths of attachment or attraction to the receptor protein. Nearly each substance under investigation demonstrates thermal stability, with the majority of them exhibiting a reduced HOMO-LUMO gap and increased softness values. A significant number of the derivatives display enhanced the affinity for binding and interactions with the receptor protein in comparison to the original drug. Moreover, a majority of the derivatives exhibit upgraded pharmacokinetic properties, rendering them innocuous for biological utilization. Furthermore, IBU-4, IBU-6, IBU-8, and IBU-11 exhibit higher binding affinity and significant non-bonding interactions when compared to IBU. In this context, the IBU8–5F19 complex exhibits the highest binding affinity among the various

Table 6
Drug likeness parameters of all IBU analogues.

Name	Lipinski (Violation)	Ghose	Veber	Egan	Muegge	Bioavailability Score	Number of H-Bond donor	Number of H-Bond acceptor
IBU	Y (0)	Y	Y	Y	Y	0.85	1	2
IBU-1	Y (0)	Y	Y	Y	Y	0.85	1	2
IBU-2	Y (0)	Y	Y	Y	Y	0.85	1	2
IBU-3	Y (0)	Y	Y	Y	Y	0.85	1	2
IBU-4	Y (0)	Y	Y	Y	Y	0.85	1	3
IBU-5	Y (0)	Y	Y	Y	Y	0.85	1	3
IBU-6	Y (0)	Y	Y	Y	Y	0.85	1	4
IBU-7	Y (0)	Y	Y	Y	Y	0.85	1	5
IBU-8	Y (0)	Y	Y	Y	Y	0.85	1	5
IBU-9	Y (1); MLOGP>4.15	N (1) WLOGP>5.6	Y	N (1); WLOGP>5.88	N (1); XLOGP3>5	0.85	1	8
IBU-10	Y (0)	Y	Y	Y	Y	0.85	1	6
IBU-11	Y (0)	Y	Y	Y	Y	0.85	1	6
IBU 12	Y (0)	N (1); WLOGP>5.6	Y	N (1); WLOGP>5.88	N (1); XLOGP3>5	0.85	1	10
IBU-13	Y (1); MLOGP>4.15	Y	Y	Y	Y	0.85	1	2
IBU-14	Y (0)	Y	Y	Y	Y	0.85	1	2
IBU-15	Y (1); MLOGP>4.15	Y	Y	Y	Y	0.85	1	2
IBU-16	Y (0)	Y	Y	Y	Y	0.85	2	3
IBU-17	Y (0)	Y	Y	Y	Y	0.85	2	3
IBU-18	Y (0)	Y	Y	Y	Y	0.56	3	4

Y= Yes, N=NO.

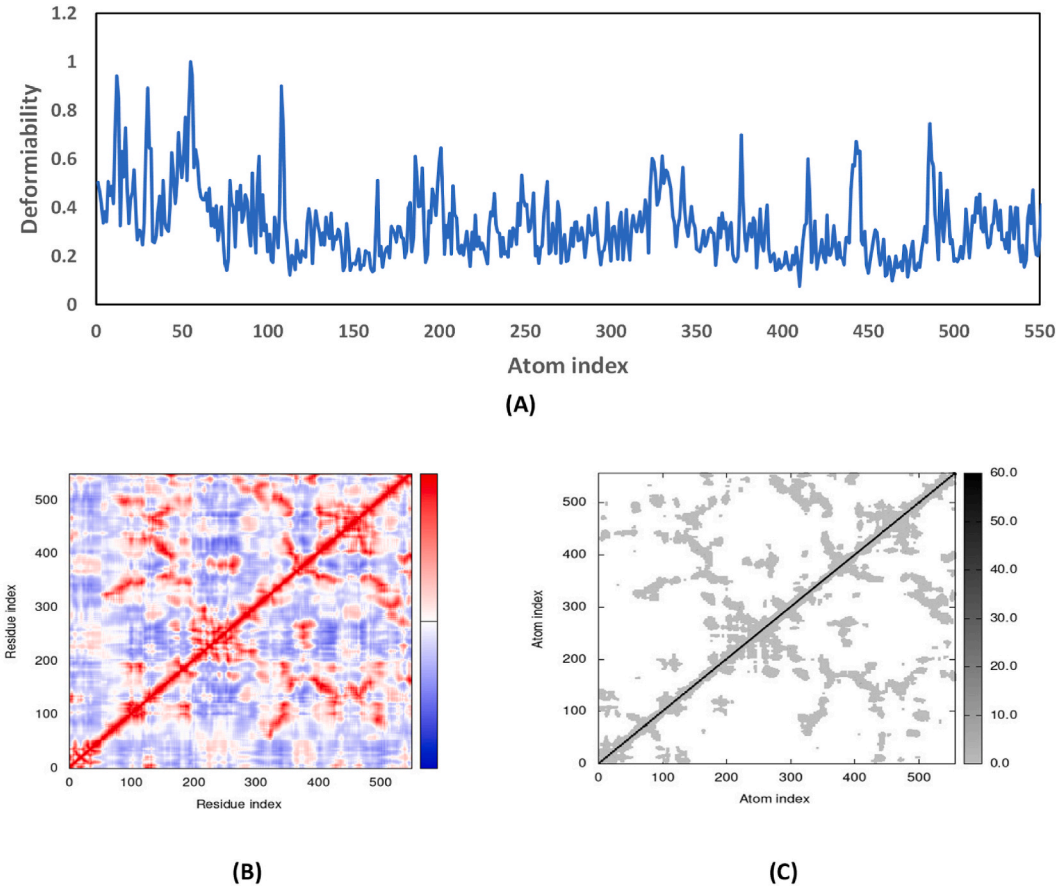

Fig. 9. Molecular dynamics simulation for receptor protein 5F19: **(A)** Deformability B-factor region of the ligand-protein interaction **(B)** Covariance map of the ligand-receptor interaction **(C)** Elastic network of the ligand-protein interaction.

complexes and remains within the binding pocket of the target protein. The outcomes indicate that the introduction of halogen has contributed to improved physicochemical and binding properties. Based on these findings, IBU-4, IBU-6, IBU-8, and IBU-11 emerge as potential candidates with promising performance. Consequently, this study holds the potential to guide the design of novel drug candidates that offer enhanced medicinal effects with reduced adverse impacts. However, further studies and experimental validations that should be conducted to assess the feasibility, safety, and efficacy of the designed drug candidates.

Funding

This research did not receive any fund.

CRediT authorship contribution statement

Mst Mahfuza Rahman: Writing – review & editing, Writing – original draft, Supervision, Methodology, Conceptualization. **Mst Farhana Afrin:** Writing – original draft, Software. **Zong Cai:** Writing – review & editing. **Gaku Ichihara:** Writing – review & editing, Investigation. **Yusuke Kimura:** Writing – review & editing. **Md Anamul Haque:** Writing – review & editing, Formal analysis. **Mir Imam Ibne Wahed:** Writing – review & editing, Software, Methodology.

Declaration of competing interest

The authors declare that they have no known competing financial interests or personal relationships that could have appeared to influence the work reported in this paper.

Appendix A. Supplementary data

Supplementary data to this article can be found online at https://doi.org/10.1016/j.heliyon.2024.e27371.

References

[1] S.K. Patel, D. Kumar, A.P. Waghmode, A. Dhabale, Solubility enhancement of ibuprofen using hydrotropic agents, Int. J. Pharm. Life Sci. 2 (2011) 542–545.
[2] R.C. Wong, S. Kang, J.L. Heezen, J.J. Voorhees, C.N. Ellis, Oral ibuprofen and tetracycline for the treatment of acne vulgaris, J. Am. Acad. Dermatol. 11 (1984) 1076–1081, https://doi.org/10.1016/S0190-9622(84)80192-9.
[3] J. Aukunuru, C. Bonepally, V. Guduri, Preparation, Characterization and Optimization of Ibuprofen Ointment Intended for Topical and Systemic Delivery, 2007. http://www.tjpr.org.
[4] E.T. Zawada, Renal consequences of nonsteroidal antiinflammatory drugs, Postgrad. Med. 71 (1982) 223–230, https://doi.org/10.1080/00325481.1982.11716077.
[5] M. Miguel-Álvarez, A. Santos-Lozano, F. Sanchis-Gomar, C. Fiuza-Luces, H. Pareja-Galeano, N. Garatachea, A. Lucia, Non-steroidal anti-inflammatory drugs as a treatment for Alzheimer's disease: a systematic review and meta-analysis of treatment effect, Drugs Aging 32 (2015) 139–147, https://doi.org/10.1007/s40266-015-0239-z.
[6] J. Wang, L. Tan, H.-F. Wang, C.-C. Tan, X.-F. Meng, C. Wang, S.-W. Tang, J.-T. Yu, Anti-inflammatory drugs and risk of alzheimer's disease: an updated systematic review and meta-analysis, J. Alzheim. Dis. 44 (2015) 385–396, https://doi.org/10.3233/JAD-141506.
[7] X. Gao, H. Chen, M.A. Schwarzschild, A. Ascherio, Use of Ibuprofen and Risk of Parkinson Disease, 2011. www.neurology.org.
[8] E.R. Rayburn, S.J. Ezell, R. Zhang, Anti-inflammatory agents for cancer therapy, Mol. Cell. Pharmacol. 1 (2009) 29–43, https://doi.org/10.4255/mcpharmacol.09.05.
[9] G.V. Joseph, V.P. Pascal, D.A. Paladini, G. Varrassi, J. V Pergolizzi, P. Dowling, A. Paladini, Ibuprofen safety at the golden anniversary: are all NSAIDs the same? A Narrative Review (2019) https://doi.org/10.6084/m9.figshare.10075727.
[10] S. Bindu, S. Mazumder, U. Bandyopadhyay, Non-steroidal anti-inflammatory drugs (NSAIDs) and organ damage: a current perspective, Biochem. Pharmacol. 180 (2020), https://doi.org/10.1016/j.bcp.2020.114147.
[11] K.E. Ward, R. Archambault, T.L. Mersfelder, Severe adverse skin reactions to nonsteroidal antiinflammatory drugs: a review of the literature, Am. J. Health Syst. Pharm. 67 (2010) 206–213, https://doi.org/10.2146/ajhp080603.
[12] Q.H. Shao, X.D. Yin, N. Zeng, Z.X. Zhou, X.Y. Mao, Y. Zhu, B. Zhao, Z.L. Li, Stevens-johnson syndrome following non-steroidal anti-inflammatory drugs: a real-world analysis of post-marketing surveillance data, Front Pediatr 10 (2022), https://doi.org/10.3389/fped.2022.896867.
[13] N.M. Davies, Clinical pharmacokinetics of ibuprofen, Clin. Pharmacokinet. 34 (1998) 101–154, https://doi.org/10.2165/00003088-199834020-00002.
[14] K.D. Rainsford, Ibuprofen: pharmacology, efficacy and safety, Inflammopharmacology 17 (2009) 275–342, https://doi.org/10.1007/s10787-009-0016-x.
[15] C. Baigent, N. Bhala, J. Emberson, A. Merhi, S. Abramson, N. Arber, J.A. Baron, C. Bombardier, C. Cannon, M.E. Farkouh, G.A. FitzGerald, P. Goss, H. Halls, E. Hawk, C. Hawkey, C. Hennekens, M. Hochberg, L.E. Holland, P.M. Kearney, L. Laine, A. Lanas, P. Lance, A. Laupacis, J. Oates, C. Patrono, T.J. Schnitzer, S. Solomon, P. Tugwell, K. Wilson, J. Wittes, O. Adelowo, P. Aisen, A. Al-Quorain, R. Altman, G. Bakris, H. Baumgartner, C. Bresee, M. Carducci, D.M. Chang, C. T. Chou, D. Clegg, M. Cudkowicz, L. Doody, Y. El Miedany, C. Falandry, J. Farley, L. Ford, M. Garcia-Losa, M. Gonzalez-Ortiz, M. Haghighi, M. Hala, T. Iwama, Z. Jajic, D. Kerr, H.S. Kim, C. Kohne, B.K. Koo, B. Martin, C. Meinert, N. Muller, G. Myklebust, D. Neustadt, R. Omdal, S. Ozgocmen, A. Papas, P. Patrignani, F. Pelliccia, V. Roy, I. Schlegelmilch, A. Umar, O. Wahlstrom, F. Wollheim, S. Yocum, X.Y. Zhang, E. Hall, P. McGettigan, R. Midgley, A. Moore, R. Philipson, S. Curtis, A. Reicin, J. Bond, M. Essex, J. Fabule, B. Morrison, L. Tive, K. Davies, F. Yau, Vascular and upper gastrointestinal effects of non-steroidal anti-inflammatory drugs: meta-analyses of individual participant data from randomised trials, Lancet 382 (2013) 769–779, https://doi.org/10.1016/S0140-6736(13)60900-9.
[16] M.E. Farkouh, J.D. Greenberg, R.V. Jeger, K. Ramanathan, F.W.A. Verheugt, J.H. Chesebro, H. Kirshner, J.S. Hochman, C.L. Lay, S. Ruland, B. Mellein, P. T. Matchaba, V. Fuster, S.B. Abramson, Cardiovascular outcomes in high risk patients with osteoarthritis treated with ibuprofen, naproxen or lumiracoxib, Ann. Rheum. Dis. 66 (2007) 764–770, https://doi.org/10.1136/ard.2006.066001.
[17] M.E. Farkouh, H. Kirshner, R.A. Harrington, S. Ruland, F.W.A. Verheugt, T.J. Schnitzer, G.R. Burmester, E. Mysler, M.C. Hochberg, M. Doherty, E. Ehrsam, X. Gitton, G. Krammer, B. Mellein, A. Gimona, P. Matchaba, C.J. Hawkey, J.H. Chesebro, Comparison of lumiracoxib with naproxen and ibuprofen in the Therapeutic Arthritis Research and Gastrointestinal Event Trial (TARGET), cardiovascular outcomes: randomised controlled trial, Lancet 364 (2004) 675–684, https://doi.org/10.1016/S0140-6736(04)16894-3.
[18] T. Grosser, S. Fries, G.A. FitzGerald, Biological basis for the cardiovascular consequences of COX-2 inhibition: therapeutic challenges and opportunities, J. Clin. Invest. 116 (2006) 4–15, https://doi.org/10.1172/JCI27291.
[19] P.C. Lo, Y.T. Tsai, S.K. Lin, J.N. Lai, Risk of asthma exacerbation associated with nonsteroidal anti-inflammatory drugs in childhood asthma: a nationwide population-based cohort study in Taiwan, Medicine (United States) (2016) 95, https://doi.org/10.1097/MD.0000000000005109.
[20] A. Chebrolu, S. Madhavan, Molecular docking study of ibuprofen derivatives as selective inhibitors of CYCLOOXYGENASE-2, Int. J. Pharma Sci. Res. 11 (2020) 6526, https://doi.org/10.13040/IJPSR.0975-8232.11(12).6526-31.
[21] J.A.H.M. Bittencourt, M.F.A. Neto, P.S. Lacerda, R.C.V.S. Bittencourt, R.C. Silva, C.C. Lobato, L.B. Silva, F.H.A. Leite, J.P. Zuliani, J.M.C. Rosa, R.S. Borges, C.B. R. Santos, In silico evaluation of ibuprofen and two benzoylpropionic acid derivatives with potential anti-inflammatory activity, Molecules 24 (2019), https://doi.org/10.3390/molecules24081476.
[22] S.P.-C. Yu, D.J. Hunter, Emerging drugs for the treatment of knee osteoarthritis, Expet Opin. Emerg. Drugs 20 (2015) 361–378, https://doi.org/10.1517/14728214.2015.1037275.
[23] M. Uzzaman, M.N. Uddin, Optimization of structures, biochemical properties of ketorolac and its degradation products based on computational studies, Daru 27 (2019) 71–82, https://doi.org/10.1007/s40199-019-00243-w.
[24] A. Onawole, M. Nasser, I. Hussein, M. Al-Marri, S. Aparicio, Theoretical studies of methane adsorption on Silica-Kaolinite interface for shale reservoir application, Appl. Surf. Sci. 546 (2021) 149164, https://doi.org/10.1016/j.apsusc.2021.149164.
[25] A.A. Olanrewaju, C.U. Ibeji, O.E. Oyeneyin, Biological evaluation and molecular docking of some newly synthesized 3d-series metal(II) mixed-ligand complexes of fluoro-naphthyl diketone and dithiocarbamate, SN Appl. Sci. 2 (2020) 678, https://doi.org/10.1007/s42452-020-2482-0.
[26] A.K. Mishra, S.P. Tewari, Density functional theory calculations of spectral, NLO, reactivity, NBO properties and docking study of Vincosamide-N-Oxide active against lung cancer cell lines H1299, SN Appl. Sci. 2 (2020), https://doi.org/10.1007/s42452-020-2842-9.
[27] M.J. Frisch, G. Trucks, H.B. Schlegel, G.E. Scuseria, M.A. Robb, J. Cheeseman, G. Scalmani, V. Barone, B. Mennucci, G.A. Petersson, H. Nakatsuji, M. Caricato, X. Li, H.P. Hratchian, A.F. Izmaylov, J. Bloino, G. Zheng, J. Sonnenberg, M. Hada, D. Fox, Gaussian 09 Revision A.1, Gaussian Inc, 2009.
[28] C. Lee, eitao Yang, R.G. Parr, Development of the Colic-Salvetti Correlation-Energy Formula into a Functional of the Electron Density, n.d. .
[29] H. Kruse, L. Goerigk, S. Grimme, Why the standard B3LYP/6-31G* model chemistry should not be used in DFT calculations of molecular thermochemistry: understanding and correcting the problem, J. Org. Chem. 77 (2012) 10824–10834, https://doi.org/10.1021/jo302156p.
[30] A.R. Allouche, Gabedita - a graphical user interface for computational chemistry softwares, J. Comput. Chem. 32 (2011) 174–182, https://doi.org/10.1002/jcc.21600.
[31] F. Azam, N.H. Alabdullah, H.M. Ehmedat, A.R. Abulifa, I. Taban, S. Upadhyayula, NSAIDs as potential treatment option for preventing amyloid β toxicity in Alzheimer's disease: an investigation by docking, molecular dynamics, and DFT studies, J. Biomol. Struct. Dyn. 36 (2018) 2099–2117, https://doi.org/10.1080/07391102.2017.1338164.
[32] M.J. Lucido, B.J. Orlando, A.J. Vecchio, M.G. Malkowski, Crystal structure of aspirin-acetylated human cyclooxygenase-2: insight into the formation of products with reversed stereochemistry, Biochemistry 55 (2016) 1226–1238, https://doi.org/10.1021/acs.biochem.5b01378.
[33] OUP accepted manuscript, Nucleic Acids Res. (2016), https://doi.org/10.1093/nar/gkw1000.
[34] N. Guex, M.C. Peitsch, SWISS-MODEL and the Swiss-PdbViewer: an environment for comparative protein modeling, Electrophoresis 18 (1997) 2714–2723, https://doi.org/10.1002/elps.1150181505.
[35] S. Dallakyan, A.J. Olson, Small-molecule library screening by docking with PyRx, in: J.E. Hempel, C.H. Williams, C.C. Hong (Eds.), Chemical Biology: Methods and Protocols, Springer New York, New York, NY, 2015, pp. 243–250, https://doi.org/10.1007/978-1-4939-2269-7_19.

[36] T. Radhika, A. Chandrasekar, V. Vijayakumar, Q. Zhu, Analysis of markovian jump stochastic cohen–grossberg BAM neural networks with time delays for exponential input-to-state stability, Neural Process. Lett. (2023), https://doi.org/10.1007/s11063-023-11364-4.
[37] A. Kistan, B.A. Benedict, S. Vasanthan, A. PremKumar, M. Kullappan, J.M. Ambrose, V.P. Veeraraghavan, G. Rengasamy, K.M. Surapaneni, Structure-Based Virtual Screening of Benzaldehyde Thiosemicarbazone Derivatives against DNA Gyrase B of Mycobacterium tuberculosis, Evidence-Based Complementary and Alternative Medicine, 2021, p. 2021, https://doi.org/10.1155/2021/6140378.
[38] S.A. Hollingsworth, R.O. Dror, Molecular dynamics simulation for all, Neuron 99 (2018) 1129–1143, https://doi.org/10.1016/j.neuron.2018.08.011.
[39] M.S. Badar, S. Shamsi, J. Ahmed, MdA. Alam, Molecular dynamics simulations: concept, Methods, and Applications (2022) 131–151, https://doi.org/10.1007/978-3-030-94651-7_7.
[40] J.R. López-Blanco, J.I. Aliaga, E.S. Quintana-Ortí, P. Chacón, IMODS: internal coordinates normal mode analysis server, Nucleic Acids Res. 42 (2014), https://doi.org/10.1093/nar/gku339.
[41] F. Cheng, W. Li, Y. Zhou, J. Shen, Z. Wu, G. Liu, P.W. Lee, Y. Tang, AdmetSAR: a comprehensive source and free tool for assessment of chemical ADMET properties, J. Chem. Inf. Model. 52 (2012) 3099–3105, https://doi.org/10.1021/ci300367a.
[42] M. Uzzaman, MdK. Hasan, S. Mahmud, A. Yousuf, S. Islam, M.N. Uddin, A. Barua, Physicochemical, spectral, molecular docking and ADMET studies of Bisphenol analogues; A computational approach, Inform. Med. Unlocked 25 (2021) 100706, 10.1016/j.imu.2021.100706.
[43] A. Daina, O. Michielin, V. Zoete, SwissADME: a free web tool to evaluate pharmacokinetics, drug-likeness and medicinal chemistry friendliness of small molecules, Sci. Rep. 7 (2017), https://doi.org/10.1038/srep42717.
[44] P. Kollman, Free Energy Calculations: Applications to Chemical and Biochemical Phenomena, 1993.
[45] Y. Liu, Is the free energy change of adsorption correctly calculated? J. Chem. Eng. Data 54 (2009) 1981, https://doi.org/10.1021/je800661q. –1985.
[46] M. Boero, K. Terakura, T. Ikeshoji, C.C. Liew, M. Parrinello, Hydrogen Bonding and Dipole Moment of Water at Supercritical Conditions, A First-Principles Molecular Dynamics Study, 2000.
[47] E.J. Lienx, Z.-R. Guo, R.-L. Li, C.-T. Su, Use of Dipole Moment as a Parameter in Drug-Receptor Interaction and Quantitative Structure-Activity Relationship Studies, n.d. .
[48] S. Saravanan, V. Balachandran, Quantum chemical studies, natural bond orbital analysis and thermodynamic function of 2,5-dichlorophenylisocyanate, Spectrochim. Acta Mol. Biomol. Spectrosc. 120 (2014) 351–364, https://doi.org/10.1016/j.saa.2013.10.042.
[49] J.I. Aihara, Reduced HOMO-LUMO gap as an index of kinetic stability for polycyclic aromatic hydrocarbons, J. Phys. Chem. A 103 (1999) 7487–7495, https://doi.org/10.1021/jp990092i.
[50] M. Uzzaman, M.K. Hasan, S. Mahmud, K. Fatema, M.M. Matin, Structure-based design of new diclofenac: physicochemical, spectral, molecular docking, dynamics simulation and ADMET studies, Inform. Med. Unlocked 25 (2021), https://doi.org/10.1016/j.imu.2021.100677.
[51] E. Scrocco, P.J. Tomasi, The Electrostatic Molecular Potential as a Tool for the Interpretation of Molecular Properties, n.d. .
[52] M.M. Matin, M. Uzzaman, S.A. Chowdhury, M.M.H. Bhuiyan, In vitro antimicrobial, physicochemical, pharmacokinetics and molecular docking studies of benzoyl uridine esters against SARS-CoV-2 main protease, J. Biomol. Struct. Dyn. 40 (2022) 3668–3680, https://doi.org/10.1080/07391102.2020.1850358.
[53] P. Politzer, J.S. Murray, Molecular Electrostatic Potentials and Chemical Reactivity, 1991.
[54] K.R. Raghi, D.R. Sherin, M.J. Saumya, P.S. Arun, V.N. Sobha, T.K. Manojkumar, Computational study of molecular electrostatic potential, docking and dynamics simulations of gallic acid derivatives as ABL inhibitors, Comput. Biol. Chem. 74 (2018) 239–246, https://doi.org/10.1016/j.compbiolchem.2018.04.001.
[55] F. Billes, I. Mohammed-Ziegler, Vibrational spectroscopy of phenols and phenolic polymers. Theory, experiment, and applications, Appl. Spectrosc. Rev. 42 (2007) 369–441, https://doi.org/10.1080/00102200701421748.
[56] E. Ramachandran, Synthesis and Characterization of Ibuprofen-CuO Nanoparticles Synthesis and Characterization of Some Drugs View Project DRS and FIP Programme of Madurai Kamaraj University View Project, 2016. www.journalspub.com.
[57] J.-W. Yang, J.-K. Choi, M.-C. Kim, H. Kim, A study of UV–vis spectroscopic and DFT calculation of the UV absorber in different solvent, Prog. Org. Coating 135 (2019) 168–175, https://doi.org/10.1016/j.porgcoat.2019.05.034.
[58] X.-Y. Meng, H.-X. Zhang, M. Mezei, M. Cui, Molecular Docking: A Powerful Approach for Structure-Based Drug Discovery, n.d. .
[59] R.C. Wade, P.J. Goodford, The role of hydrogen-bonds in drug binding, Prog. Clin. Biol. Res. 289 (1989) 433–444. http://europepmc.org/abstract/MED/2726808.
[60] A.K. Varma, R. Patil, S. Das, A. Stanley, L. Yadav, A. Sudhakar, Optimized hydrophobic interactions and hydrogen bonding at the target-ligand interface leads the pathways of Drug-Designing, PLoS One 5 (2010), https://doi.org/10.1371/journal.pone.0012029.
[61] M. Uzzaman, T. Mahmud, Structural modification of aspirin to design a new potential cyclooxygenase (COX-2) inhibitors, in: Silico Pharmacol, vol. 8, 2020, https://doi.org/10.1007/s40203-020-0053-0.
[62] M.N. Uddin, M. Uzzaman, S. Das, Md Al-Amin, MdN. Haque Mijan, Stress degradation, structural optimization, molecular docking, ADMET analysis of tiemonium methylsulphate and its degradation products, J. Taibah Univ. Sci. 14 (2020) 1134–1146, https://doi.org/10.1080/16583655.2020.1805186.
[63] M. Uzzaman, J. Shawon, Z.A. Siddique, Molecular docking, dynamics simulation and ADMET prediction of Acetaminophen and its modified derivatives based on quantum calculations, SN Appl. Sci. 1 (2019), https://doi.org/10.1007/s42452-019-1442-z.
[64] D.M. Gill, A.P. Ana, G. Zazeri, S.A. Shamir, A.M. Mahmoud, F.L. Wilkinson, M.Y. Alexander, M.L. Cornelio, A.M. Jones, The modulatory role of sulfated and non-sulfated small molecule heparan sulfate-glycomimetics in endothelial dysfunction: absolute structural clarification, molecular docking and simulated dynamics, SAR analyses and ADMET studies, RSC Med. Chem. 12 (2021) 779–790, https://doi.org/10.1039/d0md00366b.
[65] A.M. Davis, R.J. Riley, Predictive ADMET studies, the challenges and the opportunities, Curr. Opin. Chem. Biol. 8 (2004) 378–386, https://doi.org/10.1016/j.cbpa.2004.06.005.
[66] L.L.G. Ferreira, A.D. Andricopulo, ADMET modeling approaches in drug discovery, Drug Discov. Today 24 (2019) 1157–1165, https://doi.org/10.1016/j.drudis.2019.03.015.
[67] Y. Han, J. Zhang, C.Q. Hu, X. Zhang, B. Ma, P. Zhang, In silico ADME and toxicity prediction of ceftazidime and its impurities, Front. Pharmacol. 10 (2019), https://doi.org/10.3389/fphar.2019.00434.
[68] C.M. Nisha, A. Kumar, P. Nair, N. Gupta, C. Silakari, T. Tripathi, A. Kumar, Molecular docking and in silico admet study reveals acylguanidine 7a as a potential inhibitor of β -secretase, Adv Bioinformatics 2016 (2016), https://doi.org/10.1155/2016/9258578.
[69] R.B. van Breemen, Y. Li, Caco-2 cell permeability assays to measure drug absorption, Expet Opin. Drug Metabol. Toxicol. 1 (2005) 175–185, https://doi.org/10.1517/17425255.1.2.175.
[70] A.E. Rettie, J.P. Jones, Clinical and toxicological relevance OF CYP2C9: drug-drug interactions and pharmacogenetics, Annu. Rev. Pharmacol. Toxicol. 45 (2004) 477–494, https://doi.org/10.1146/annurev.pharmtox.45.120403.095821.
[71] M.J. Stubbins, L.W. Harries, G. Smith, M.H. Tarbit, C.R. Wolf, Genetic Analysis of the Human Cytochrome P450 CYP2C9 Locus, vol. 6, Pharmacogenet Genomics, 1996. https://journals.lww.com/jpharmacogenetics/Fulltext/1996/10000/Genetic_analysis_of_the_human_cytochrome_P450.7.aspx.
[72] M.L. Amin, P-glycoprotein inhibition for optimal drug delivery, Drug Target Insights 2013 (2013) 27–34, https://doi.org/10.4137/DTI.S12519.
[73] S. Wang, Y. Li, J. Wang, L. Chen, L. Zhang, H. Yu, T. Hou, ADMET evaluation in drug discovery. 12. Development of binary classification models for prediction of hERG potassium channel blockage, Mol. Pharm. 9 (2012) 996–1010.
[74] A. Lagunin, A. Stepanchikova, D. Filimonov, V. Poroikov, PASS: prediction of activity spectra for biologically active substances, Bioinformatics 16 (2000) 747–748, https://doi.org/10.1093/bioinformatics/16.8.747.
[75] D.A. Filimonov, A.A. Lagunin, T.A. Gloriozova, A. V Rudik, D.S. Druzhilovskii, P. V Pogodin, V. V Poroikov, Prediction of the biological activity spectra of organic compounds using the pass online web resource, Chem Heterocycl Compd (N Y). 50 (2014) 444–457, https://doi.org/10.1007/s10593-014-1496-1.
[76] W. Wei, S. Cherukupalli, L. Jing, X. Liu, P. Zhan, Fsp3: a new parameter for drug-likeness, Drug Discov. Today 25 (2020) 1839–1845, https://doi.org/10.1016/j.drudis.2020.07.017.
[77] S. Tian, J. Wang, Y. Li, D. Li, L. Xu, T. Hou, The application of in silico drug-likeness predictions in pharmaceutical research, Adv. Drug Deliv. Rev. 86 (2015) 2–10, https://doi.org/10.1016/j.addr.2015.01.009.

[78] L. Guan, H. Yang, Y. Cai, L. Sun, P. Di, W. Li, G. Liu, Y. Tang, ADMET-score-a comprehensive scoring function for evaluation of chemical drug-likeness, Medchemcomm 10 (2019) 148–157, https://doi.org/10.1039/C8MD00472B.
[79] C.A. Lipinski, F. Lombardo, B.W. Dominy, P.J. Feeney, Experimental and computational approaches to estimate solubility and permeability in drug discovery and development settings1PII of original article: S0169-409X(96)00423-1. The article was originally published in Advanced Drug Delivery Reviews 23 (1997) 3–25.1, Adv. Drug Deliv. Rev. 46 (2001) 3–26, https://doi.org/10.1016/S0169-409X(00)00129-0.
[80] A.K. Ghose, V.N. Viswanadhan, J.J. Wendoloski, A knowledge-based approach in designing combinatorial or medicinal chemistry libraries for drug discovery. 1. A qualitative and quantitative characterization of known drug databases, J. Comb. Chem. 1 (1999) 55–68, https://doi.org/10.1021/cc9800071.
[81] D.F. Veber, S.R. Johnson, H.Y. Cheng, B.R. Smith, K.W. Ward, K.D. Kopple, Molecular properties that influence the oral bioavailability of drug candidates, J. Med. Chem. 45 (2002) 2615–2623, https://doi.org/10.1021/jm020017n.
[82] W.J. Egan, K.M. Merz, J.J. Baldwin, Prediction of drug absorption using multivariate statistics, J. Med. Chem. 43 (2000) 3867–3877, https://doi.org/10.1021/jm000292e.
[83] I. Muegge, S.L. Heald, D. Brittelli, Simple selection criteria for drug-like chemical matter, J. Med. Chem. 44 (2001) 1841–1846, https://doi.org/10.1021/jm015507e.
[84] J.T.S. Coimbra, R. Feghali, R.P. Ribeiro, M.J. Ramos, P.A. Fernandes, The importance of intramolecular hydrogen bonds on the translocation of the small drug piracetam through a lipid bilayer, RSC Adv. 11 (2020) 899–908, https://doi.org/10.1039/d0ra09995c.
[85] M.-Q. Zhang, B. Wilkinson, Drug discovery beyond the 'rule-of-five, Curr. Opin. Biotechnol. 18 (2007) 478–488, https://doi.org/10.1016/j.copbio.2007.10.005.